Use of optically detected magnetic resonance to correlate germanium electron centres with UV absorption bands in x-ray irradiated germanosilicate glasses

2000 J. Phys.: Condens. Matter 12 8309

(http://iopscience.iop.org/0953-8984/12/38/307)

J. Phys.: Condens. Matter **12** (2000) 8309–8319. Printed in the UK PII: S0953-8984(00)14662-4

Use of optically detected magnetic resonance to correlate germanium electron centres with UV absorption bands in x-ray irradiated germanosilicate glasses

D P Poulios†, N P Bigelow† and J P Spoonhower†‡

† Department of Physics and Astronomy, University of Rochester, Rochester, NY, 14627, USA
‡ Eastman Kodak Research Laboratories, Rochester, NY, USA

Received 13 June 2000

Abstract. The relationship between paramagnetic defect centres and UV absorption bands simultaneously generated by ionizing radiation in Ge-doped SiO_2 glass is investigated using magneto-optical techniques. A sample of 7.0 mol% Ge-doped SiO_2 was exposed to x-ray radiation, which resulted in the formation of absorption bands centred at 4.4 eV and 5.7 eV as well as electron spin resonance (ESR) signals attributed to the Ge(1) and Ge(2) defects. To isolate paramagnetic contributions to the induced optical absorption, the magnetic circular dichroism absorption (MCDA) spectrum was measured at several different temperatures over the range 2.00–6.21 eV. The optically detected magnetic resonance (ODMR) spectrum was then obtained at 4.42 eV via microwave-induced changes in the MCDA signals in order to unambiguously correlate this optical transition with a particular ESR signal. The ODMR data indicate that the Ge(1) centre is responsible for this absorption band, providing the first unequivocal correlation of ESR and optical properties for this defect. In addition, evidence of a weakly absorbing paramagnetic defect, that appears to be related to the Ge(2) centre, was found at 5.65 eV.

1. Introduction

Germanosilicate glasses and germanium-doped silica fibres have been extensively studied for over a decade, mostly because of their photosensitive properties and utility in producing Bragg gratings and other optical devices. Despite the intense research efforts, however, the precise mechanisms responsible for the photosensitive effect remain unclear. Many researchers have focused on elucidating the defect photochemistry in the glass structure as a possible means of explaining this effect. In the most widely accepted model, photorefractive index changes in Ge-doped SiO_2 induced by exposure to ultraviolet light or ionizing radiation are brought about by the presence of germanium oxygen-deficient defect centres (GODCs) in the glass network [1]. Two such defects thought to play significant roles in the photosensitive phenomenon are the neutral oxygen monovacancy (NOMV) and the neutral oxygen divacancy (NODV or Ge^{2+}), both of which have electronic transitions in the vicinity of 5.16 eV [2]. NOMV and NODV are known to be photobleached by UV radiation via one- and two-photon effects [3, 4], respectively, although the exact mechanism by which the NODV bleaching occurs is subject to considerable debate [3–6]. These photobleaching processes are known to lead to the production of several broad UV absorption bands, the most notable of which are centred at 6.5 eV, 5.8 eV and 4.5 eV [5, 7, 8].

Also produced in these processes are a number of paramagnetic point defects, which may play a significant role in UV-induced index changes, the most relevant being the two

0953-8984/00/388309+11$30.00

varieties of germanium trapped electron centres (GECs), known as Ge(1) and Ge(2), and the GeE′ centre. Ge(1) is believed to be a substitutional Ge tetrahedron with four silicon atoms as the next nearest neighbours [9] that has trapped an electron donated by either an NODV or a bridging oxygen [3, 4]. Various experiments have shown that this defect centre can be produced by either two-photon absorption of excimer laser light (KrF, XeCl or ArF) [3, 4, 10], single-photon absorption of light from a KrCl excimer lamp [6] or by ionizing radiation such as x- or γ-rays [9, 11]. A similar structure has been proposed for the Ge(2) defect (electron trapped at Ge tetrahedron with one Ge and three Si atoms as next nearest neighbours) [9], although there is significant recent evidence to suggest the Ge(2) is actually an NODV which has trapped a hole [6, 12]. The GeE′ centre, consisting of a threefold coordinated Ge with an unpaired electron, is readily produced by single-photon scission of the metal–metal bond of an NOMV [2, 13]; there is also evidence that GeE′ can be formed by the photobleaching of GECs [3].

Assignment of these defects to particular optical absorption features has proven difficult for several reasons. One is the somewhat formless nature of the optical absorption spectrum of irradiated germanosilicate glasses caused by the overlap of the induced absorption bands with the GODCs. This overlap makes accurate spectral separation of absorptions quite difficult. Electron spin resonance (ESR) spectroscopy, often of great use in identifying defects in solids, suffers a similar difficulty when the GECs and the GeE′ centre are simultaneously present, as their spectra are considerably entangled. In an effort to correlate these germanium-related paramagnetic species with induced absorption bands, concomitant measurements of ESR and optical absorption spectra have been conducted as a function of annealing temperature. This technique has been used to attribute the 6.5 eV, 5.8 eV and 4.5 eV bands to GeE′, Ge(2) and Ge(1) [14, 15], respectively, but it must be noted that it does not provide unambiguous correlation between a given defect's ESR and absorption spectra, particularly when multiple centres with broad overlapping bands are present.

To correlate these properties in a direct manner for the Ge(1) and Ge(2) centres, we first measured the magnetic circular dichroism absorption (MCDA) spectrum of an x-ray irradiated 7.0 mol% Ge-doped SiO_2 sample over the range 2.07–6.21 eV at various temperatures to establish which bands are paramagnetic. This technique also provided spectral separation of the induced paramagnetic bands from those of the GODCs and other diamagnetic defects. We then examined the optically detected magnetic resonance (ODMR) spectrum associated with MCDA signal extrema via microwave-induced changes in the MCDA signal. Using this ODMR technique, we were able to establish unequivocal correlations between optical transitions and specific ESR spectra; this has not been accomplished previously. Identification of the defects seen in the ODMR spectra was possible by making comparisons with ESR data taken on a conventional spectrometer.

2. Experiment

2.1. Sample preparation

The germanosilicate glass used in the experiment was hewn from a section of 7.0 mol% GeO_2, 93.0 mol% SiO_2 single-mode fibre preform fabricated using the vapour axial deposition (VAD) method. The preform was first cut into a 10 mm × 5 mm × 2 mm slab and polished on two sides. According to the glass specifications, the germanium concentration varied by less than 1% from the centre to the edges of the sample. The sample was then exposed to radiation from a 2.4 kW tungsten anode x-ray tube (50 kV, 48 mA) at room temperature in order to create defects throughout the glass network. The defect concentration was periodically measured through

double numerical integration of ESR spectra and comparison to a standard sample containing a known number of Si E′ centres. Irradiation was halted once the induced spin density of the germanosilicate sample became saturated ($\sim 10^{17}$ spins cm^{-3}).

2.2. MCDA and ODMR theory

MCD is an effect common to all matter whereby the application of a static uniform magnetic field to a material induces an asymmetry in the optical densities for right- and left-hand circularly polarized light (herein referred to as A_+ and A_-, respectively) propagating parallel or antiparallel to the field. In simplest terms, the MCD phenomenon can be viewed as a sum of three separate manifestations of the Zeeman effect: (1) unresolved field-induced splitting of a degenerate ground or excited state, (2) mixing of nearby states by the magnetic field and (3) population differentials between ground state magnetic sublevels [16]. The first two contributions, often grouped into the single term 'diamagnetic effect', are temperature independent and linear in field strength; the third term depends strongly upon the temperature and is referred to as the paramagnetic term. It is then possible to write the MCDA signal as

$$\Delta A = DA_{para}(B, T) + DA_{dia}(B) \tag{1}$$

where DA_{para} is the paramagnetic term, DA_{dia} is the diamagnetic term, B is the magnetic field strength and T is the temperature [17]. For systems with degenerate ground states, the paramagnetic term tends to dominate the MCDA spectrum, particularly at low temperatures. Use of low temperatures in MCDA spectroscopy is especially advantageous when a system has a complicated optical absorption spectrum consisting of many overlapping bands, and one wishes to differentiate paramagnetic contributions from diamagnetic ones.

The paramagnetic part of the MCDA signal is also useful for the detection of magnetic resonance in the ground state. For $S^{1/2}$ systems (such as the GECs), the differential absorption may be written as the simple expression

$$\Delta A \propto \tanh\left(\frac{g u_B H}{2kT}\right) \tag{2}$$

where it is assumed that the equilibrium population distribution amongst the ground state Kramers doublet follows Boltzmann statistics, and that the diamagnetic contributions to the MCDA signal may be ignored [18]. Equation (2) indicates that MCDA can be used as a sensitive probe of the spin temperature of a given system's ground state. Observation of ODMR is then carried out by measuring perturbations in the MCDA signal (and, hence, the spin temperature) brought about by driving spin transitions between ground state sublevels with resonant microwaves of sufficient power to overcome the spin–lattice relaxation rate. This optical method of detecting spin resonance transitions offers several advantages over conventional ESR techniques, the most significant being that optical rather than microwave quanta are used in the detection process (providing up to a $\sim 10^4$ gain in sensitivity), and that the optical properties of a given defect are unambiguously correlated with its spin resonance spectrum. It should be noted that the selectivity of the ODMR method allows for the disentanglement of the optical and ESR properties of simultaneously present defects provided only that these properties are not identical.

2.3. Experimental apparatus and techniques

MCDA spectra were recorded at temperatures of 4.2 K and 1.6 K. The MCD spectrometer used consisted of a 30 W deuterium lamp focused onto the entrance slit of a single grating 0.25 m monochromator having a bandwidth of less than 3 nm over the range 2.07–6.21 eV. The output

light was linearly polarized by a Glan–Taylor polarizing prism and directed through a 42 kHz photoelastic modulator, which alternately produced right- and left-hand circularly polarized light at its fundamental frequency. The sample was mounted in a variable-temperature helium cryostat with four-way optical access outfitted with a superconducting magnet capable of operating at 1.8 T with a homogeneity of 1 part in 10^4 over 1 cm^3. The polarization-modulated light was then focused onto the sample by a set of computer-controlled motorized lenses designed to account for chromatic aberration. Light transmitted by the sample was then trained on a photomultiplier tube connected to a feedback circuit which varied the tube voltage in order to keep the DC light signal constant as a function of wavelength. A lock-in amplifier referenced to the modulator frequency measured the differential absorption of the two polarizations of light; the ratio of the lock-in signal to the DC light signal yields a quantity proportional to $\Delta A = A_- - A_+$, the difference in optical densities for right and left circularly polarized light [19]. A computer scanned the spectrometer in 0.5 nm steps and recorded the lock-in voltage, DC light signal and tube voltage in order to obtain the full MCDA spectrum. A long-pass filter was used for the range 3.45–6.21 eV to filter out second-order UV light from the monochromator.

Optical absorption spectra in the range 2.26–6.21 eV were measured at room temperature before and after irradiation using a commercial two-beam spectrophotometer. The spectral bandwidth was kept at 3 nm, and the spectra were adjusted for instrument response by baseline subtraction.

To obtain ODMR spectra below 5.18 eV, the deuterium lamp–monochromator system was replaced by a 150 W high-pressure mercury lamp equipped with a 0.1 m monochromator for improved light throughput. Unmodulated 24.1 GHz (K-band) microwaves from a 600 mW klystron were then coupled into a cylindrical microwave sample cavity using a coaxial antenna. As the magnetic field was scanned, the computer recorded negative changes in the MCDA signal caused by resonant microwave-driven transitions between ground state Zeeman sublevels as a function of field strength. Acquisition of ODMR spectra above 5.18 eV was carried out in much the same manner, the only difference being that a deuterium lamp filtered by a 220 nm interference filter was used as a light source to compensate for the monochromator's weak light throughput in the deep UV. The bandwidth of the interference filter was 10 nm and transmitted approximately 0.1% of incident light at 5.28 eV and 6.27 eV. All ODMR spectra were acquired at a sample temperature of 1.6 K. For purpose of comparison, ESR spectra were also recorded on a separate commercial unit at 300 K using 9.6 GHz (X-band) microwaves at power level of 13.6 mW and a field modulation of 100 kHz. The signal amplitude and spin density were measured at several different microwave power levels to ensure that the sample was not being saturated. The magnetic field sweeps for both the ESR and ODMR spectrometers were calibrated using diphenylpicrylhydrazyl (DPPH, $g = 2.0036$) as a standard.

3. Results and discussion

3.1. ESR results

Prior to x-ray exposure, the Ge-doped glass sample shows no measurable ESR activity. After 15 hours of x-irradiation at 300 K, an ESR signal (shown in figure 1) emerges which closely resembles the spectra of the GECs previously reported in the literature [6, 11, 20, 21]. The spectrum shown in figure 1 contains overlapping ESR contributions from both the Ge(1) and Ge(2) centres. In an effort to resolve the composite irradiated germanosilicate glass ESR spectrum into its individual components, researchers have conducted various isochronal annealing experiments. Several results emerge from these studies. One is the correlation of

particular features of the GEC ESR signal with individual defects, such as the local minimum at $g = 1.9934$, attributed to the Ge(1) defect, and the minimum at $g = 1.9869$, related to the Ge(2) centre [11, 20]. Another significant finding is that there is some overlap between the Ge(1) and Ge(2) signals above $g = 2.000$ [22] but the two are otherwise spectrally separate. It is interesting to note that the typical ESR pattern of the GeE′ centre [2, 11] is absent from figure 1, indicating that the x-irradiation did not photochemically produce this defect in any measurable quantity. This finding contrasts with experiments conducted with excimer laser light, where it has been suggested that GECs are produced in the initial stages of irradiation and subsequently transformed to GeE′ centres with continued exposure [3].

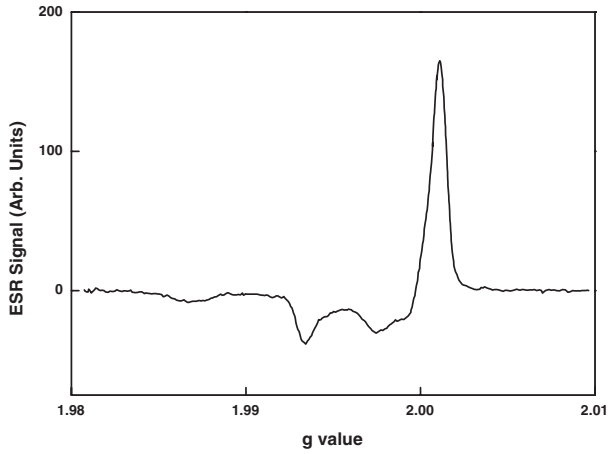

Figure 1. ESR spectra of x-irradiated Ge-doped silica glass measured at 300 K.

3.2. Optical absorption and MCDA results

The optical absorption spectra of the glass sample prior to x-irradiation is shown in figure 2(a), with the only notable detail being the strong GODC absorption band centred at 5.16 eV. Also shown in figure 2(a) is the post-irradiation absorption spectrum. As is evident in the plot, it is difficult to ascertain the precise shape and location of the peaks of the radiation-induced bands due to their considerable overlap with the broad NODV and NOMV optical transitions. The strategy most frequently employed to obtain these quantities in irradiated Ge-doped SiO_2 systems is to fit multiple Gaussian peaks to the induced absorption spectrum, as is shown in figure 2(b). Since no evidence of the GeE′ centre was seen in the ESR data, the induced absorption spectrum was fitted with three Gaussian functions (representing Ge(1), Ge(2) and the GODCs) rather than the usual four. In this figure, the best fit to the data shows the growth of absorption bands centred around 4.73 eV and 6.06 eV, while the initial 5.16 eV absorption band is depleted; these results are consistent with what is generally found in the literature [3–6, 8, 23]. While this fitting procedure is useful in that it provides a rough estimate of the optical properties of the induced defects, the process is obviously prone to considerable error, particularly the choice of initial conditions for the fits. One must also account for the possibility that one or more diamagnetic species could be induced in the glass that would obviously be undetectable by ESR spectroscopy; these defects would of course be ignored in the fitting process.

MCDA spectroscopy is uniquely suited to circumvent this difficulty as the Ge(1) and

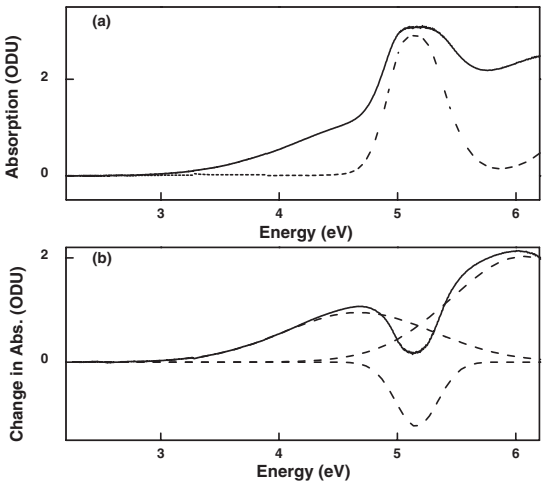

Figure 2. (a) Absorption spectra of unirradiated (dashed line) and irradiated (solid line) Ge-doped silica glass. (b) Radiation-induced change in optical absorption (solid line) with Gaussian components (dashed lines). Both sets of data were measured at 300 K.

Ge(2) centres provide significant paramagnetic contributions while the NOMV and NODV show only comparably weak diamagnetic signals; thus, the transitions are easily spectrally separated using their respective temperature dependences. The MCDA spectra of the irradiated and unirradiated (inset) sample measured at 1.6 and 4.2 K with a field strength of 1.8 T are presented in figure 3. The spectra were corrected for diamagnetic signal contributions from the fused quartz cryostat windows as well as for zero-field baseline effects. Prior to irradiation, the MCDA spectrum at 4.2 K is featureless except for a negative-going band peaking at 5.16 eV that is clearly attributable to singlet–singlet GODC transitions. Lowering the temperature to 1.6 K produces no change in the GODC MCDA signal strength, providing further evidence to support the long-standing assumption that the GODCs are diamagnetic in nature. Despite a careful search, no evidence of the singlet–triplet NODV transition believed to occur at 3.8 eV [6] could be found. This could due to the band's weak oscillator strength as well as its diamagnetic character. Upon completion of the x-irradiation, growth of an MCDA band peaking at 4.42 eV is observed, as well as a slight decrease in the depth of the GODC signal, indicating that these centres undergo a small degree of photobleaching. It is quite clear upon viewing the spectra that paramagnetic centres are responsible for the 4.42 eV band, as the peak signal strength increases by a factor of approximately 1.8 upon lowering the temperature from 4.2 K to 1.6 K. No other paramagnetic signals were as readily apparent in figure 3, possibly due to the spectrometer's low light throughput in the deep UV, which required the use of greater photomultiplier tube voltages to produce measurable signals. This effect significantly degraded the signal-to-noise ratio of the spectra above 5.50 eV and made it difficult to discern any structure, and may also have obscured weak absorption bands overlapping with the GODCs in this range.

3.3. ODMR and tagged MCDA results

The upper trace of figure 4 shows a plot of the ODMR spectra of the x-irradiated sample measured at 4.42 eV. The technique used for obtaining ODMR spectra involved coupling fixed-frequency CW microwaves into the sample cavity and monitoring the MCDA signal as the field strength was increased; the signal dips in figure 4 indicate where a particular defect's

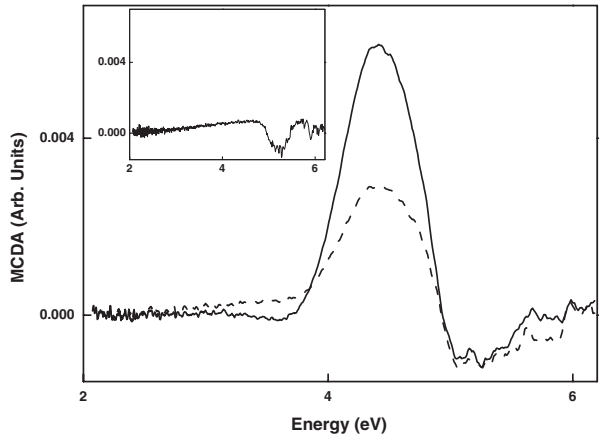

Figure 3. MCDA spectra of irradiated glass measured at 4.2 K (dashed line) and 1.6 K (solid line) at 1.8 T. Inset shows MCDA spectrum of unirradiated glass measured at 4.2 K, 1.8 T. *X* and *Y* scales are identical on both plots.

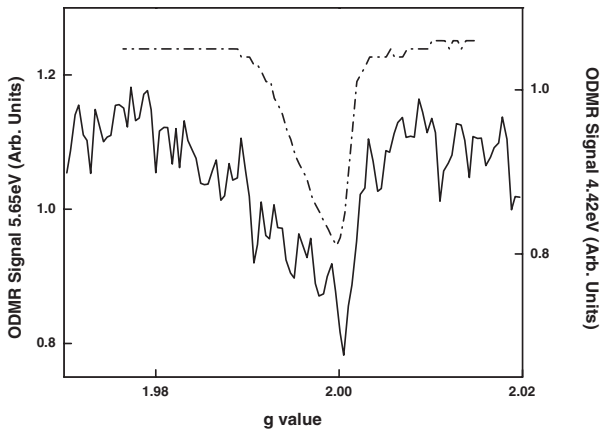

Figure 4. ODMR spectra measured at 4.42 eV (dashed line) and 5.65 eV (solid line) at 1.6 K.

ground state splitting is resonant with the frequency of the microwave field. The ODMR data shows that a spin resonance signal peaking at $g = 2.000$ is directly associated with the induced absorption band at 4.42 eV, providing conclusive evidence that the GECs are indeed responsible for at least a portion of the induced absorption spectrum at this energy. ODMR was also attempted at 5.65 eV to account for the possibility that a defect with a weak paramagnetic absorption at this energy might be obscured by the high signal noise and thus would not be apparent in the MCDA spectra of figure 3. As was mentioned previously, a 220 nm (5.65 eV) interference filter was employed rather than the monochromator to increase light throughput. The 5.65 eV ODMR signal is shown in the bottom trace of figure 4. It is similar to the 4.42 eV trace in that it has a peak at $g = 2.000$, but also contains additional significant signal contributions below $g = 1.990$; these results indicate that the GECs also absorb in the deep UV range transmitted by the filter. There are several possible explanations for the presence of the $g = 2.000$ signal at 5.65 eV. One is that the 4.42 eV band is broad enough to overlap with

the filter transmission range so that it 'leaks' into the 5.65 eV ODMR signal, while another possibility is that the defect responsible for the 4.42 eV band has another separate higher-energy transition. Although several reports, including recent studies of defect-free irradiated germanosilicate glasses by Chiodini *et al* [21], have supported the latter possibility, the current data does not permit exclusion of either scenario. It seems the most likely explanation for the additional breadth of the 5.65 eV ODMR signal is that a defect unrelated to the 4.42 eV band weakly absorbs in this region. It is impossible to deduce where the peak oscillator strength of this defect lies based on the data presented here, but considering the relative weakness of the MCDA signal in the range 5.0–6.2 eV, it is reasonable to ascribe this defect to one of the broad absorption bands located at higher energies (6.2–7.5 eV) found in deep UV spectroscopy studies [7]. Part of the ODMR signal at 5.65 eV could then be directly related to the 'tail' of one of these bands found at higher energies.

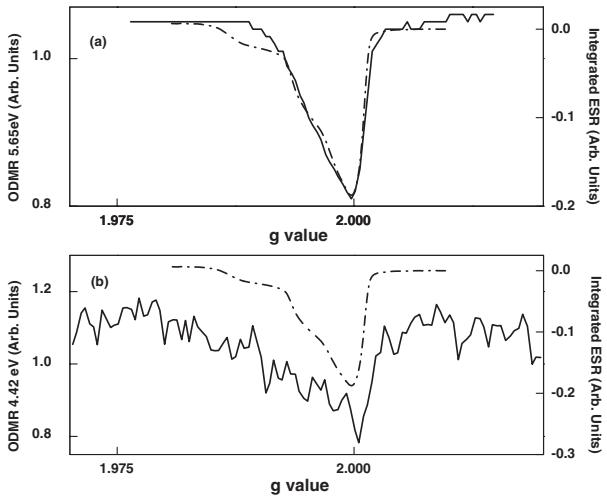

Figure 5. (a) ODMR spectrum measured at 4.42 eV, 1.6 K (solid line) versus integrated ESR spectrum (dashed line) measured at 300 K. (b) ODMR spectrum measured at 5.65 eV, 1.6 K (solid line) versus integrated ESR (dashed line).

The question of which defect is responsible for these optical transitions can be addressed by comparing the ODMR data to the ESR data of figure 1. Because ODMR directly records the absorption of microwave power as a function of magnetic field strength rather than the corresponding derivative (as in conventional ESR spectroscopy), direct comparisons to the ESR data are tedious unless the latter is first integrated. Figure 5(a) shows a comparison of the integrated GEC ESR spectrum displayed in figure 1 to the ODMR spectrum measured at 4.42 eV shown in figure 4. The two techniques show excellent agreement, as it is clear from figure 5(a) that both the ODMR and ESR spectra share a peak at $g = 2.000$ and have similar bandshapes despite the great difference in temperature. Perhaps the most significant aspect of this comparison is the lack of a shoulder in the vicinity of $g = 1.985$ in the ODMR spectrum, suggesting that the Ge(2) centre plays no role in the optical transition at 4.42 eV; thus, the Ge(1) defect is solely responsible for the radiation-induced paramagnetic absorption here. The ODMR results also indicate that the composite ESR spectrum of the GECs above $g = 1.990$ is dominated by Ge(1). This assertion is supported by the work of Anoikin *et al*, who were able to isolate the Ge(1) ESR signal in Ce^{3+}-doped germanosilicate glass; though they did not supply particular g-values for the Ge(1) centre, the ESR spectrum shown in their work

closely resembles the composite GEC spectrum shown in figure 1 [24]. A direct comparison of the 5.65 eV ODMR spectrum and the integrated GEC ESR spectrum is shown in figure 5(b). Although the poor signal-to-noise ration precludes rigorous assessment of the features of the ODMR spectrum, intriguing possibilities emerge from the comparison. The signal dip at approximately $g = 2.000$ seems to indicate the presence of the Ge(1) defect; however, the nonzero ODMR signal below $g = 1.990$ invites correlation with the Ge(2) shoulder of the integrated ESR spectrum, a feature undetected in the 4.42 eV ODMR. Unfortunately, lack of a clean ODMR signal prevents definite assignments here, and further studies are clearly necessary to ascertain which defects are present.

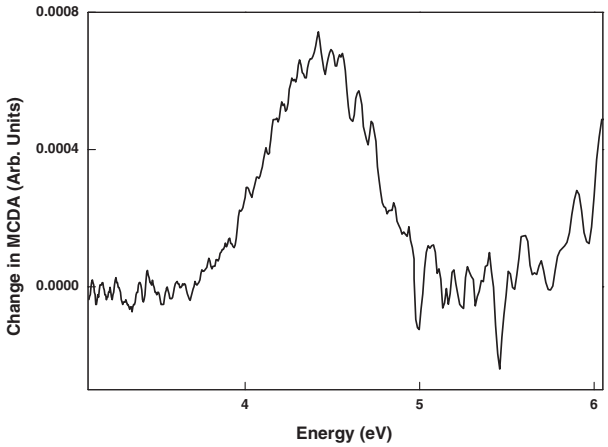

Figure 6. Tagged MCDA spectrum of Ge(1) centre measured at 1.6 K.

The ODMR results may also be used to further elucidate the optical properties of the induced defects. By tuning the magnetic field to a particular spin resonance transition and measuring the MCDA signal as the wavelength is varied, it is possible to trace out an ODMR excitation spectrum for a given defect. This method, known as 'tagged MCDA' [17], serves a number of purposes. It identifies all optical transitions associated with a paramagnetic defect and effectively isolates its individual MCDA spectrum from the total MCDA, which is particularly useful when separating overlapping bands belonging to different defects [17]. It is also possible to use tagged MCDA to estimate the peak position and width of an absorption band, though it is not necessarily a reliable measure of bandshape [25]. The tagged MCDA spectrum shown in figure 6 was obtained by setting the magnetic field to the peak of the 4.42 eV ODMR band and measuring the MCDA spectrum over the range 3.11–6.00 eV with the microwave power on; the microwave power was sufficiently attenuated so that no sample heating was detectable. This measurement was then repeated with the microwave power off; the difference between the two spectra yielded the tagged MCDA spectrum. No tagging data were available above 6.00 eV due to the extremely high signal-to-noise ratio that resulted after subtraction. The preferred 'digital lock-in' tagging method described by Spaeth *et al* [26], which employs low-frequency modulation of the microwave power to induce changes in the MCDA, was ineffective in this case, probably because of the typically long spin–lattice relaxation times found in irradiated glasses [27]. Since the tagging technique effectively removes all diamagnetic signals from the measurement, it allowed the bandshape of the Ge(1) centre to be accurately measured without concern of distortion from the GODC absorption. The tagged MCDA spectrum for Ge(1) shows that the band extends from 3.5 eV to approximately

5.3 eV. Furthermore, the close similarity in bandshape between the MCDA of figure 3 and the tagged spectrum indicates that the Ge(1) centre is responsible for all the paramagnetic absorption in the range 2.01–5.3 eV; similar claims may not be made for absorption bands above 5.3 eV using the tagging technique due to high signal noise. Attempts to tag the MCDA spectra with the field set to the Ge(2) ESR line were unsuccessful, as the signal noise was simply too great to produce reliable data. Thus, no further information about the nature of the absorption above 5.3 eV could be obtained from these experiments.

An obvious inconsistency with the standard defect model for irradiated germanosilicate glasses emerges from the ODMR and tagged MCDA results. These techniques firmly establish that the Ge(1) centre is responsible for a broad absorption in the 4.4–4.7 eV range as had been previously suggested. However, a discrepancy is found regarding the optical properties of the Ge(2) centre. Recall that the Ge(2) defect is considered to be correlated with a broad band centred in the 5.7–6.1 eV range, the optical properties of which are determined by a Gaussian fitting procedure. The Gaussian fit to the optical absorption data shown in figure 2(b) suggests that the 6.06 eV absorption ascribed to the Ge(2) defect in the standard model has the largest peak oscillator strength in the range measured, yet the MCDA spectrum clearly shows considerably weaker paramagnetic absorption from 5.0 to 6.2 eV than at 4.42 eV. The lack of a strong paramagnetic signal in this range indicates that the defect or defects responsible for the majority of the optical absorption are likely diamagnetic in nature; therefore, the Ge(2) defect does not correlate well with the optical properties suggested by the standard model. One possible explanation for this is that the simple three-band deconvolution of the induced optical absorption is inadequate, and that one or more induced diamagnetic bands are responsible for the majority of the optical absorption above 5 eV. Further research is currently under way to clarify these assignments, including studies of UV-irradiated germanosilicate glasses; experiments with irradiated hydrogen-loaded germanosilicates are also in progress.

4. Conclusions

Paramagnetic defects are created in 7.0 mol% Ge-doped SiO_2 glass via prolonged x-irradiation along with a number of optical absorption bands in the range 2.01–6.21 eV. ESR data suggest Ge(1) and Ge(2) centres are formed in the greatest quantities, while the GeE′ defect is experimentally undetectable. MCDA spectra of the irradiated glass measured at 4.2 K and 1.6 K show a large paramagnetic band at 4.42 eV, and much weaker paramagnetic absorption above 5.0 eV. Comparison of ODMR and ESR measurements indicate that the 4.42 eV absorption is due to the Ge(1) centre, and tagged MCDA was used to positively identify all optical transitions associated with this defect. These results are in accordance with the widely accepted model for Ge(1) in irradiated germanosilicate glasses. Lack of strong paramagnetic absorption above 5.0 eV indicates that diamagnetic defects are responsible for the bulk of the optical density in this region, contradicting the widely accepted notion that the Ge(2) centre is the dominant absorbing centre here. Comparison of ODMR and ESR data shows that the Ge(2) centre may in fact absorb at 5.65 eV, which suggests its peak oscillator strength lies in the deeper UV range of the spectrum. This result considered with the MCDA data indicate the simple three-defect model in irradiated Ge-doped SiO_2 systems must be augmented.

Acknowledgments

The authors gratefully acknowledge T Erdogan and A Heaney for samples used in these experiments. This work was supported by NSF DMR-9612267.

References

[1] Atkins R M and Mizrahi V 1992 *Electron. Lett.* **28** 1743
[2] Hosono H, Abe Y, Kinser D L, Weeks R A, Muta K and Kawazoe H 1992 *Phys. Rev.* B **46** 11 445
[3] Nishii J, Fukumi K, Yamanaka H, Kawamura K, Hosono H and Kawazoe H 1995 *Phys. Rev.* B **52** 1661
[4] Fujimaki M, Yagi K, Ohki Y, Nishikawa H and Awazu K 1996 *Phys. Rev.* B **53** 9859
[5] Essid M, Albert J, Brebner J L and Awazu K 1999 *J. Non-Cryst. Solids* **246** 39
[6] Fujimaki M, Watanabe T, Katoh T, Kasahara T, Miyazaki N, Ohki Y and Nishikawa H 1998 *Phys. Rev.* B **57** 3920
[7] Neustruev V B 1994 *J. Phys.: Condens. Matter* **6** 6901
[8] Shigemura, Kawamoto H Y, Nishii J and Takahashi M 1999 *J. Appl. Phys.* **85** 3413
[9] Tsai T E, Griscom D L and Friebele E J 1987 *Diff. Defect Data* **53–54** 469
[10] Nishii J, Kitamura N, Yamanaka H, Hosono H and Kawazoe H 1995 *Opt. Lett.* **20** 1184
[11] Friebele E J, Griscom D L and Siegel G H Jr 1974 *J. Appl. Phys.* **45** 3424
[12] Anoikin E V, Guryanov A N, Gusovskii D D, Mashinskii V M, Miroshnichenko S I, Neustruev V B, Tikhomirov V A and Zverev Y B 1991 *Sov. Lightwave Commun.* **1** 123
[13] Hosono H, Kawazoe H and Nishii J 1996 *Phys. Rev.* B **53** 11 921
[14] Friebele E J and Griscom D L 1985 *Defects in Glasses (MRS Symp. Proc. 61)* ed F L Galeener, D L Griscom and M J Weber (Pittsburgh, PA: Materials Research Society) p 319
[15] Neustruev V B, Dianov E M, Kim V M, Mashinsky V M, Romanov M V, Guryanov A N, Khopin V F and Tikhomirov V A 1989 *Fiber Integrated. Optics.* **8** 143
[16] Geschwind S 1972 *Electron Paramagnetic Resonance* (New York: Plenum) p 386
[17] Spaeth J M and Lohse F M 1990 *J. Phys. Chem. Solids* **51** 861
[18] Stephens P J 1976 *Adv. Chem. Phys.* **25** 197
[19] Drake A F 1986 *J. Phys. E: Sci. Instrum.* **19** 170
[20] Fujimaki M, Katoh T, Kasahara T, Miyazaki N and Ohki Y 1999 *J. Phys.: Condens. Matter* **11** 2589
[21] Chiodini N, Meinardi F, Morazzoni F, Paleari A and Scotti R 1999 *Phys. Rev.* B **60** 2429
[22] Guryanov A N, Kim V M, Mashinsky V M, Neustruev V B, Romanov M V, Tikhomirov V A and Khopin V F 1990 *Proc. Gen. Phys. Inst. Moscow* **23** 94
[23] Essid M, Brebner J L, Albert J and Awazu K 1998 *J. Appl. Phys.* **84** 4193
[24] Anoikin E V, Guryanov A N, Gusovsky D D, Dianov E M, Mashinsky V M, Miroshnichenko S I, Neustruev V B, Tikhomirov V A and Zverev Y B 1992 *Nucl. Instrum. Methods Phys.* B **65** 392
[25] Spaeth J M 1987 *Electronic Magnetic Resonance of the Solid State* (Ottawa: Canadian Society for Chemistry) p 503
[26] Ahlers F J, Lohse F, Spaeth J M and Mollenauer L F 1983 *Phys. Rev.* B **28** 1249
[27] Bricis D, Ozols J, Rogulis U, Trokss J, Meise W and Spaeth J M 1992 *Solid State Commun.* **81** 745